J Solution Chem (2010) 39: 1099–1112
DOI 10.1007/s10953-010-9568-z

Solubility of Thiophene-, Furan- and Pyrrole-2-Carboxaldehyde Phenylhydrazone Derivatives in 2.82 mol·L^{-1} Aqueous DMSO at 298.15 K, Inhibition of Lymphoproliferation and Tubulin Polymerization: A Study Based on the Scaled Particle Theory

Ysaías J. Alvarado · Melchor Álvarez-Mon · Joanna Baricelli · José Caldera-Luzardo · Néstor Cubillán · Gladys Ferrer-Amado · Manzur Hassanhi · Yovani Marrero-Ponce · Victoria Mancilla · Miguel A. Rocafull · María Esther San Antonio-Sánchez · José Ojeda-Andara · Luz E. Thomas

Received: 24 September 2009 / Accepted: 10 March 2010 / Published online: 20 August 2010

Abstract In this work, the solubilities of nine phenylhydrazone derivatives in water and in 2.82 mol·L^{-1} aqueous DMSO at 298.15 K, expressed on the molar fraction scale, are reported. The estimated value of the standard Gibbs energy for transferring the solute from water to 2.82 mol·L^{-1} DMSO, $\Delta G^0_{W\rightarrow mix}$, for each system, indicates that it is a spontaneous

Y.J. Alvarado (✉) · G. Ferrer-Amado
Departamento de Investigación en Tecnología de los Materiales y el Ambiente (DITeMA), Instituto Venezolano de Investigaciones Científicas (IVIC), Avenida 74 con calle 14A, Maracaibo, República Bolivariana de Venezuela
e-mail: yalvaradofec@yahoo.com

M. Álvarez-Mon · M.E. San Antonio-Sánchez
Laboratorio de Inmunología y Oncología, Departamento de Medicina, Facultad de Medicina, Universidad de Alcalá, Alcalá de Henares, Madrid, España

J. Baricelli · M.A. Rocafull · L.E. Thomas
Laboratorio de Fisiología Molecular, Centro de Biofísica y Bioquímica, Instituto Venezolano de Investigaciones Científicas (IVIC), Carretera Panamericana Km 11, Apartado 21827, Caracas 1020-A, República Bolivariana de Venezuela

Y.J. Alvarado · J. Caldera-Luzardo · N. Cubillán · V. Mancilla · J. Ojeda-Andara
Laboratorio de Electrónica Molecular(LEM), Departamento de Química, Facultad Experimental de Ciencias, La Universidad del Zulia, Ap. 526, Grano de Oro, Módulo No. 2, Maracaibo, Estado Zulia, República Bolivariana de Venezuela

M. Hassanhi
Laboratorio de Farmacología, Facultad de Medicina, La Universidad del Zulia, Maracaibo, Estado Zulia, República Bolivariana de Venezuela

Y. Marrero-Ponce
Laboratorio de Diseño de Fármacos, Departamento de Farmacia, Centro de Química Bio-activa, Universidad Central de las Villas, Santa Clara, Cuba

process. Some of the phenylhydrazone derivatives inhibited the induction of T lymphocyte proliferation by phytohaemagglutinin (PHA) but only DPCT and NPCF efficiently inhibited Guinea pig brain tubulin polymerization. Scaled Particle Theory (SPT) was used to interpretate solubility and biological activity results. Based on the results we suggested that the difference in the work of cavity creation $\Delta\Delta G_c$, associated with the transfer of the phenylhydrazone derivatives from water to 2.82 mol·L^{-1} aqueous DMSO, is the dominant factor in the magnitude of $\Delta G^0_{W\to mix}$. The later quantity was considered to be an indirect measurement of the hydrophobic character of these derivatives, and it can be used to interpret the biological results.

Keywords Solubility · SPT · Tubulin polimerization · Lymphoproliferation · Phenylhydrazone derivatives

1 Introduction

The hydrazones have proved to be important molecules due to their potential antitumor, antileukemic, antipsychotic, antiseptic, antifungal and antibacterial activities [1–4]. Morgan and co-workers have proposed that the presence of a nitro group in the ortho-position and a hydrazone bridge appear to be important conditions for interactions with surface tumor markers via electrostatic/non-covalent binding with the arginine, serine/threonine and, cysteine moieties [4]. Even though the exact mechanism of anticancer activity for these molecular systems is still unknown, the biological action of such compounds could be related to their exceptional electronic properties and hydrophobicity [4, 5]. In fact, the hydrophobic effect is the major driving force involved in the binding of drugs to their receptor target [6].

Data about the chemical processes in solution, of hydrazone compounds, are quite scarce, probably due to their hydrophobic character and their low solubility in common organic solvents [5, 7]. Nevertheless, these data are very important for understanding the role that the specific and nonspecific solvent–solute interactions play in the binding between these compounds and their target sites [8]. In order to overcome this difficulty, DMSO is often used as co-solvent to improve the solubility of organic compounds which are not soluble in common aprotic solvents and water, since most of the compounds screened for biological activities are more soluble in dimethylsulfoxide (DMSO) than in water (W) at room temperature [1–4]. In addition, this solvent is frequently used for the *in vivo* administration and *in vitro* experimentation of several water-insoluble compounds [9].

There is a growing interest in our group in the study of thermodynamics of solvation and its relationship with biological activity, especially the anticancer activity. Previously, we have described the relationship between the DNA-phenylhydrazone association constant, the antiproliferative activity on the breast tumor line MDA231 and the Gibbs energy of cavity creation in a medium within the Scaled-Particle Theory framework [10].

Now, in this paper we report the experimental equilibrium solubility of the thiophene-2-, furan-2- and pyrrole-2-carboxaldehyde phenylhydrazone, 4-phenylhydrazone and 2,4-dinitrophenylhydrazone derivatives (henceforth referred to as PCT, PCF, PCP, NPCT, NPCF and NPCP, DPCT, DPCF and DPCP, respectively, see Fig. 1) at 298.15 K in water and in 2.82 mol·L^{-1} aqueous DMSO. From these data, the Gibbs energies of solution ΔG^0_i and Gibbs energies of transfer from water to the mixed solvents $\Delta G^0_{W\to mix}$ were estimated for each compound. Additionally, the anti-inflammatory activity of a selected group of these compounds was evaluated by measuring the inhibitory activity on T-lymphocyte proliferation activated by phytohemagglutinin (PHA) [11], and the inhibition of Guinea pig brain

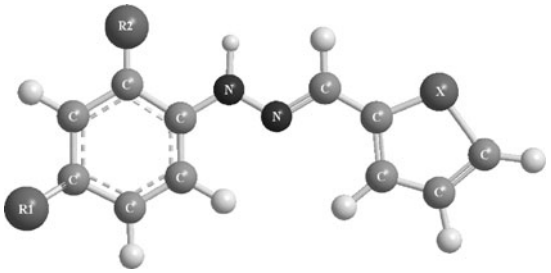

	X	R1	R2
PCF	O	-H	-H
NPCF	O	$-NO_2$	-H
DPCF	O	$-NO_2$	$-NO_2$
PCP	NH	-H	-H
NPCP	NH	$-NO_2$	-H
DPCP	NH	$-NO_2$	$-NO_2$
PCT	S	-H	-H
NPCT	S	$-NO_2$	-H
DPCT	S	$-NO_2$	$-NO_2$

Fig. 1 Structure and nomenclature of phenylhydrazone derivatives of furan, pyrrole and thiophene

tubulin polymerization [12, 13]. Tubulin is an accepted target for treatments against cancer [14]. The results obtained in this work were analyzed and interpreted in terms of the scaled particle theory (SPT) (i.e., in terms of the work to create the cavity in the solution and the molar solute-solvent interaction energy). It is important to mention that this theory has been used previously to study liquid solutions and proteins [15–17] and to evaluate the interaction of phenylhydrazone with DNA [10].

2 Experimental Section

2.1 General Considerations

The phenylhydrazone derivatives (see Fig. 1) used in this work were synthecized following a method developed by our group and reported elsewhere [7, 10]. The method is based on the solvent free or aqueous condensation assisted by microwave irradiation of phenylhydrazine, 4-nitrophenylhydrazine, or 2,4-dinitrophenyl-hydrazine with the corresponding furan, pyrrole and thiophene carboxaldehyde. Water was sterilized and deionized in all the cases. Dimethylsulfoxide (DMSO) was purchased from Aldrich and rigorously dried by appropriate drying agents, fractionally distilled and collected and stored over molecular sieves [7, 18–22]. DMSO was chosen as co-solvent in order to improve the solubility of phenylhydrazone derivatives in water. Solubility studies were carried out by using aqueous DMSO (20% V/V, 2.82 mol·L^{-1}).

2.2 Solubility and Thermodynamics of Solution

The solubility determination was carried out following the procedure reported by our group [10], based on the spectrometrical method of Zielenkiewicz and co-workers [23], using an UV-Vis-NIR spectrophotometer (Shimadzu UV-3101PC) with a diode array detector thermoelectrically thermostated at 298.15 K in a cell holder (Shimadzu TCC-260). The experiments were repeated at least five times for each solubility value. The reproducibilities, as relative standard deviations, were better than 2%. The standard Gibbs energies ΔG_i^0 were calculated from the molar fraction χ_2 of each solute in a saturated solution using the following equation

$$\Delta G_i^0 = -RT \ln \chi_{2,i} \tag{1}$$

where R is the gas constant, T is the absolute temperature, and i represents the medium: water (W) or 2.82 mol·L^{-1} aqueous DMSO (mix).

From these solubility measurements of phenylhydrazone derivatives at 298.15 K in 2.82 mol·L^{-1} aqueous DMSO mixture, the Gibbs energy of transfer $\Delta G^0_{W\to mix}$ from water as reference solvent to the mixed solvents was estimated as [24]

$$\Delta G^0_{W\to mix} = \Delta G^0_{mix} - \Delta G^0_{W} = RT \ln\left(\frac{\chi_{2,W}}{\chi_{2,mix}}\right) \tag{2}$$

The Ben-Naim standard Gibbs energy change, $\Delta G^*_{W\to mix}$, upon transfer of a solute molecule from a fixed position in water to a fixed position in 2.82 mol·L^{-1} aqueous DMSO at constant pressure, temperature and composition, was calculated by the relation [16, 17, 25–29]

$$\Delta G^*_{W\to mix} = \Delta G^0_{W\to mix} + RT \ln\left(\frac{V_{mix}}{V_W}\right) \tag{3}$$

Here, V_W and V_{mix} are the molar volume at 298.15 K of water ($V_W = 18.07$ cm^3·mol^{-1}) and mean molar volume of 2.82 mol·L^{-1} aqueous DMSO ($V_{mix} = 20.74$ cm^3·mol^{-1}), respectively. In this work V_{mix} was estimated as $V_{mix} = \chi_W V_W + \chi_{DMSO} V_{DMSO}$ supposing that they formed an ideal solution. In consequence, the term $RT \ln(V_{mix}/V_W) = 0.341$ kJ·mol^{-1}.

2.2.1 *Scaled-Particle Theory Calculation of* $\Delta G^*_{W\to mix}$

The standard Gibbs energy change $\Delta G^*_{W\to mix}$ in this model is divided in two subprocesses: (a) creation of a cavity to accommodate the solute molecule in the medium and (b) turning on the solute–solvent interactions. Their magnitudes can be estimated by [26, 29]

$$\Delta G^*_{W\to mix} = [\Delta G_c(mix) - \Delta G_c(W)] + [G_{int}(mix) - G_{int}(W)] = \Delta\Delta G_c + \Delta G^{\theta}_{int} \tag{4}$$

where ΔG_c is the work of cavity creation, and G_{int} is the Gibbs energy of solute–solvent interaction. The Gibbs energy required to create a cavity in each medium was calculated by Eq. 5 following the scaled-particle theory (SPT)

$$\Delta G_c = RT\left[K_0 + K_1\left(\frac{\sigma_2}{\sigma_1}\right) + K_2\left(\frac{\sigma_2}{\sigma_1}\right)^2 + K_3\left(\frac{\sigma_2}{\sigma_1}\right)^3\right] \tag{5}$$

where σ_2 and σ_1 are the hard-sphere diameters of solute and solvent, $K_0 = -\ln(1-\xi)$, $K_1 = \Phi = 3\xi/(1-\xi)$, $K_2 = \Phi(\Phi+2)/2$, $K_3 = \xi p V_1/RT$, with p as the hydrostatic pressure over the liquid, V_1 the molar volume of the medium, and ξ as the volume packing density of pure solvent, that can be mathematically expressed as: $\xi_i = \pi N_A \sigma_i^3/6V_i$, and it is defined as the ratio of the physical volume of a mole of solvent molecules to the molar volume of the solvent with N_A as Avogadro's number. For water and DMSO, we used $\sigma_W = 2.80 \times 10^{-8}$ cm, $V_W = 18.07$ cm^3·mol^{-1}, $\xi_W = 0.383$, $\sigma_{DMSO} = 4.91 \times 10^{-8}$ cm, $V_{DMSO} = 71.37$ cm^3·mol^{-1} and $\xi_{DMSO} = 0.523$ as suggested by Graziano [16, 29, 30]. It is well-known that the estimation of G_c from SPT strongly depends on the values of solute and solvent hard-sphere diameters. These quantities are very important and affect the magnitude of others parameters as, for example, ξ. Graziano selected $\sigma = 2.80 \times 10^{-8}$ cm ($\xi = 0.383$) since this value is closer to the location of the first peak in the oxygen-oxygen radial distribution function of water determined experimentally by means of x-ray and neutron-scattering measurements (i.e., the effective size of two H-bonded water molecules is 2.80×10^{-8} cm), and also because the corresponding reported values of G_c are reliable in comparison to those obtained by means of computer simulations in several water models [30].

Although the 2.82 mol·L^{-1} aqueous DMSO calculations were made by assuming an ideal solution, the mean hard-sphere diameter of the mixed solvent systems ($\sigma_{mix} = 2.91 \times 10^{-8}$ cm) was estimated as $\sigma_{mix} = \chi_W\sigma_W + \chi_{DMSO}\sigma_{DMSO}$ and $\xi_{mix} = 0.373$ calculated with $\xi_{mix} = \pi N_A\sigma_{mix}^3/6V_{mix}$.

The solute–solvent interaction energy G_{int}^{θ} can be considered as the sum of two standard energy contributions [16, 17, 31, 32], G_{sp}^{θ} and G_{nsp}^{θ}, due to solute–solvent specific (donor–acceptor interactions) and nonspecific (van der Waals forces) interactions, respectively,

$$G_{int}^{\theta} = G_{sp}^{\theta} + G_{nsp}^{\theta} \tag{6}$$

and for ΔG_{int}^{θ}

$$\Delta G_{int}^{\theta} = \Delta G_{sp}^{\theta} + \Delta G_{nsp}^{\theta} = (G_{sp}^{\theta}(\text{mix}) - G_{sp}^{\theta}(\text{W})) + (G_{nsp}^{\theta}(\text{mix}) - G_{nsp}^{\theta}(\text{W})) \tag{7}$$

It is important to recognize that the energy contribution from the chemical interactions G_{sp}^{θ} is difficult to estimate. In contrast, the second term is considered as the sum of energy contributions from dipole–dipole (G_{dd}), induction (G_{ind}), dispersion (G_{disp}), dipole–quadrupole ($G_{\mu Q}$), and quadrupole-quadrupole (G_{QQ}) solvent–solute interactions [31–34]. In this work the energy contribution in each medium was estimated using Eq. 8, and neglecting the quadrupolar and dipole–quadrupole forces yields

$$G_{nsp}^{\theta} = -N_A\left(\frac{16(\varepsilon_1 - 1)\xi}{(2\varepsilon_1 + 1)\sigma_2^3}\right)\mu_2^2 - \frac{N_A}{2}\left(\frac{48(\varepsilon_1 - 1)\xi k_B T}{(2\varepsilon_1 + 1)\sigma_2^3}\right)\alpha_2 - \frac{3N_A}{2}\left(\frac{I_1 I_2}{I_1 + I_2}\right)\frac{\alpha_1\alpha_2}{d^6} \tag{8}$$

where the first, second and third terms correspond to the contributions from intermolecular interactions of dipole–dipole, induction and dispersion (London) types, respectively, and the parameters k_B, ε, I, μ and α are the Boltzmann constant, dielectric constant, vertical ionization energy, dipole moment and electronic polarizability, respectively (the subscript 1 and 2 represent the solvent and solute), and d is the distance between two hard-spheres that is defined as $d = (\sigma_1 + \sigma_2)/2$. The mixture parameters α and I for the 2.82 mol·L^{-1} aqueous DMSO were empirically estimated as $\alpha_1 = \chi_W\alpha_W + \chi_{DMSO}\alpha_{DMSO}$ and $I_1 = \chi_W I_W + \chi_{DMSO} I_{DMSO}$. We have treated the 2.82 mol·L^{-1} (1:18 DMSO:W mole ratio) aqueous DMSO as an ideal mixture with a continuum dielectric since the results of neutron diffraction have shown that the tetrahedral hydrogen bonding network of water remains largely intact at the 1:20 mole ratio [35]. Consequently, the solution can be characterized by its mean parameters (volume, dielectric constant, etc.).

Alternatively, as proposed by Graziano [16], the values of ΔG_{sp}^{θ} can be empirically estimated from

$$\Delta G_{int}^{\theta} = \Delta G_{W\to mix}^{*} - \Delta\Delta G_c \tag{9}$$

The difference between ΔG_{int}^{θ} and ΔG_{nsp}^{θ} can give information about the chemical interactions (weak hydrogen bonds or weak electron donor–acceptor complexes) that occur between the solute and DMSO molecules in the hydration shell. In the systems where the specific solute–solvent component of the van der Waals ΔG_{sp}^{θ} is very small or negligible, Eq. 4 can be rewritten as

$$\Delta G_{W\to mix}^{*} = \Delta\Delta G_c + \Delta G_{nsp}^{\theta} \tag{10}$$

Table 1 Quantum mechanical calculation results of the vertical ionization energy (I/kJ$\times 10^{21}$), polarizability (α/esu$\times 10^{23}$) and dipole moment ($|\mu|$/Debye) of the phenylhydrazones under study

Compound	I	α	$\|\mu\|$
PCF	1.089	2.785	3.775
NPCF	1.185	3.547	8.764
DPCF	1.232	3.673	8.993
PCP	1.048	2.842	0.749
NPCP	1.141	3.431	7.732
DPCP	1.184	3.732	8.472
PCT	1.090	3.012	2.280
NPCT	1.185	3.547	8.777
DPCT	1.233	3.893	8.727

2.2.2 *Theoretical Calculation of Vertical Ionization Energy, Dipole Moment, Electronic Polarizability and Molecular Volume*

With the purpose of estimating G^{θ}_{nsp} in Eq. 8, several quantities for phenylhydrazones were calculated with quantum mechanical methods (I, μ, α and V). The geometrical structures were optimized considering Cs symmetry, using Density Functional Theory with the B3LYP functional and 6-311++G(3d,3p) basis set. The vertical ionization energy (I) was calculated through the strategy proposed by Librando and Alparone based on the energy difference between a neutral molecule and its cation [36]. The dipole moment (μ) and electronic polarizability (α) were calculated by analytical methods. The hard-sphere diameter of each solute σ_2 was calculated using Suppan's equation [37], i.e. $\sigma_2 = 2(3V_2/4\pi N_A)^{1/3}$, where V_2 is the corresponding molar volume in the gas phase calculated by Monte Carlo integration of an envelope space of electron density with a contour value of 0.001 atomic units [38]. All calculations were carried out in the Gaussian 2003 quantum chemistry package [39]. The results obtained for these molecular systems are shown in Table 1.

2.3 Preparation of Primary Human T-lymphocytes, Lymphoproliferation and Measurement of Inhibitory Effects of Phenylhydrazone Derivatives on T-lymphocyte Proliferation

The experimental protocol was reviewed and approved by the Human Experimentation Committee. Written informed consent was obtained from each and every subject. Preparation of primary human T lymphocytes: Heparinized human peripheral blood (40 mL) was obtained from normal healthy volunteers. Human peripheral blood mononuclear cells were isolated by the Ficoll-Hypaque gradient centrifugation method as described previously [40, 41]. The cells resuspended in RPMI-1640, counted and their viability checked by trypan blue exclusion [40–42]. Cells were cultured (duplicate) in RPMI-1640 medium supplemented with 10% heat-inactivated fetal calf serum and antibiotics. 50 µL (1000 cells$\cdot\mu$L^{-1}) aliquots of cell suspensions were placed in a 96-well microtitre, followed by incubation with PHA (10 µg$\cdot$mL^{-1}) (Sigma-Aldrich) and phenylhydrazone derivatives (10^{-5} mol$\cdot$L^{-1}) for 5 days. Incubations were at 310 K in a humidified CO_2 atmosphere [42]. The concentration of DMSO in these studies for each solution was less than 1% V/V. Cyclosporine A was used as negative and positive. Subsequently, 20 µL of tritiated thymidine (1 mCi$\cdot$mL^{-1}) was added to each well. After 24 h of incubation, the cells were harvested on fiberglass filters by an automatic harvester system. Radioactivity in the filters was measured

by scintillation counting (Wallac Perkin Elmer) [43, 44]. Cell proliferation is determined by estimating the incorporation of [3H]thymidine into DNA, a process which is closely related to underlying changes in the cell number. The inhibitory activity IA(%) of compounds on T-lymphocyte proliferation was determined by us as [11]

$$\mathrm{IA} = \frac{CPM(\text{control}) - CPM(\text{drug})}{CPM(\text{control})} \cdot 100 \tag{11}$$

2.4 Preparation of Pure Tubulin

All operations were at 275 K unless otherwise indicated. Guinea pig brain tubulin was prepared by three cycles of polymerization–depolymerization followed by chromatography on DEAE-sepharose FF [12]. The eluted tubulin, depleted of microtubule-associated proteins, was concentrated by ultrafiltration, adjusted to 0.05 mol·L^{-1} 2-(N-morpholino) ethanesulfonic acid (MES)–NaOH, pH = 6.8, 0.25 mmol·L^{-1} $MgCl_2$, 0.5 mmol·L^{-1} EGTA, 3.4 mol·L^{-1} glycerol, and 0.2 mmol·L^{-1} GTP (30% glycerol buffer), and stored at 301 K at a concentration of 2 mg·mL^{-1}.

2.5 Microtubule Assembly Assay

Tubulin, at 273 to 275 K in 30% glycerol buffer, was supplemented with 6 mmol·L^{-1} $MgCl_2$ and 1 mmol·L^{-1} GTP and used within a concentration range of 1 to 1.5 mg·mL^{-1}. The final buffer composition was 0.05 mol·L^{-1} MES–NaOH, pH = 6.8, 6.25 mmol·L^{-1} $MgCl_2$, 0.5 mmol·L^{-1} EGTA, 3.4 mol·L^{-1} glycerol, and 1.2 mmol·L^{-1} GTP, and was called the assembly buffer. Polymerization was initiated by a temperature shift from 283 to 310 K [12] in a thermostated 1-cm light path cell and was monitored turbidimetrically at 350 nm with a spectrophotometer Synergy HT (Biotek Instruments), equipped with a thermostatically-controlled cell holder. The concentration of drug stock solutions in DMSO solution was 2×10^{-3} mol·L^{-1}. These compounds were added to the tubulin solution before polymerization. The content of DMSO in all cases was less than 2% by volume. In this study colchicine was used as a control of assembly inhibition. The IC_{50} value for colchicine in this assay is near to 1.4 μmol·L^{-1}, which agrees with the reported value [45].

3 Results and Discussion

3.1 Solubility and Thermodynamics of Solution

The solubility, on the mole fraction scale, determined by UV-Vis spectrometry for each compound in water χ_2(W) and 2.82 mol·L^{-1} DMSO χ_2(mix) at 293.15 K, is presented in Table 2. As it can be seen, independently of the heteroatom in the heterocyclic ring, the solubility diminishes with incremental increases of the number of nitro groups on the phenyl ring moiety. Also, the solubilities of compounds in 2.82 mol·L^{-1} DMSO are markedly larger than in water. The values of the Gibbs energy for the dissolution process in water ΔG^0_{W} and in 2.82 mol·L^{-1} aqueous DMSO mixture $\Delta G^0_{\mathrm{mix}}$ are large and positive for each studied compound (see Table 2), and their magnitude increases with the increment of the substitution of H by a nitro group on the phenyl ring—i.e., the highest values of $\Delta G^0_{\mathrm{mix}}$ were obtained for the hydrazone derivatives containing the 2,4-dinitrophenyl ring. In the same table in the

Table 2 Solubilities of phenylhydrazones (molar fraction) and thermodynamic quantities (kJ·mol^{-1}) associated with the dissolution process in water (W), in 2.82 mol·L^{-1} DMSO(mix), and the transfer of solute from W to the mixture, inhibitory activity IA(%) of phenylhydrazone derivatives on T-lymphocyte proliferation stimulated with PHA, and inhibitory effects (IC_{50}/μmol·L^{-1}) on tubulin polymerization

Compound	$\chi_2(W)\times10^7$	$\chi_2(mix)\times10^5$	ΔG^0_W	ΔG^0_{mix}	$-\Delta G^0_{W\to mix}$	$-\Delta G^*_{W\to mix}$ [a]	IA(%)	IC_{50}
PCF	5.73	2.28	35.63	26.50	9.13	9.47 (9.34)		
NPCF	1.72	1.05	38.61	28.43	10.18	10.52 (9.42)	25.00	0.58 ± 0.03
DPCF	0.14	0.17	44.88	32.97	11.90	12.24 (9.99)	37.50	
PCP	5.86	5.95	35.57	24.12	11.45	11.80 (9.97)		
NPCP	1.73	2.09	38.60	26.71	11.88	12.22 (10.14)		
DPCP	0.16	0.36	44.43	31.06	13.37	13.71 (10.60)		
PCT	5.19	7.40	35.87	23.58	12.30	12.64 (10.05)	37.50	inactive
NPCT	1.68	3.08	38.66	25.75	12.91	13.25 (10.11)	18.75	inactive
DPCT	0.07	0.24	46.41	32.05	14.36	14.70 (10.65)	62.50	0.52 ± 0.03

[a]Values in parenthesis were calculated with Eq. 10

sixth and seventh columns are listed the corresponding values of $\Delta G^0_{W\to mix}$ and $\Delta G^*_{W\to mix}$ calculated by means of Eqs. 2 and 3.

From these results it is clear that the transfer from water to 2.82 mol·L^{-1} aqueous DMSO at 298.15 K is a spontaneous process in all considered systems, as expected, due clearly to the high solubility of the compounds in 2.82 mol·L^{-1} DMSO with respect to water. Interestingly, the absolute values of $\Delta G^*_{W\to mix}$ have a increasing trend with σ_2 (see Table 3). This means that the transfer of a molecule from a fixed position in liquid water to a fixed position in 2.82 mol·L^{-1} aqueous DMSO is mainly governed by the molecular size of the solute. As shown in Table 2 and 3, the absolute value of $\Delta G^*_{W\to mix}$ decreases in the following order: phenylhydrazone derivatives (PCF < PCP < PCT); *p*-nitrophenylhydrazone derivatives (NPCF < NPCP < NPCT) and 2,4-dinitrophenylhydrazone derivatives (DPCF < DPCP < DPCT). Consequently, we suggest that the value of $\Delta G^*_{W\to mix}$ may be considered as a direct measurement of the interactions between the solute and DMSO molecules in the hydration shell, resulting in an indirect measurement of the hydrophobic character for each phenylhydrazone derivative.

Table 3 collects the values obtained for the work of cavity creation ΔG_c, the nonspecific components of the van der Waals forces G^θ_{nsp}, the values of $\Delta\Delta G_c$, the solute–solvent van der Waals interaction energy ΔG^θ_{int}, and the values of ΔG^θ_{nsp} associated with the transfer of the nine phenylhydrazone derivatives from water to 2.82 mol·L^{-1} DMSO at 298.15 K. From this table it can be seen that the work for cavity creation ΔG_c in water is greater than in 2.82 mol·L^{-1} DMSO. The observed increment in $\Delta\Delta G_c$ is a consequence of the small hard-sphere diameter of water in comparison to the mean hard-sphere diameter of a binary solvent system, and is also due to the higher volume packing density in water in relation to the mixture ($\xi_W > \xi_{mix}$). It is known that ΔG_c has an inverse trend with σ of the solvent and a direct increasing trend with ξ [26, 28]. These results indicate that the excluded volume effect is significant and could be the cause of the low solubility of these derivatives in water. As a consequence $\Delta\Delta G_c$ is negative, which favors the transfer from water to 2.82 mol·L^{-1} DMSO. In fact, when $\Delta\Delta G_c$ was correlated with the hard-sphere diameter of the solute σ_2 in this non homologous family of compounds, a linear trend was found with a coefficient of correlation of -0.9999 ± 0.0084 and $p < 0.0001$ (graph omitted for simplicity).

Table 3 Hard-sphere diameter of phenylhydrazones ($\sigma_2 \times 10^8$ cm) and thermodynamic quantities (kJ·mol^{-1}) associated with the dissolution process in water (W) and in 2.82 mol·L^{-1} DMSO(mix), and the transfer of solute from W to mix

	σ_2	ΔG_c(W)	ΔG_c(mix)	$-\Delta\Delta G_c$	ΔG^{θ}_{int}	$-G^{\theta}_{nsp}$(W)	$-G^{\theta}_{nsp}$(mix)	ΔG^{θ}_{nsp}	$-\Delta G^{\theta}_{sp}$
PCF	7.66	80.60	71.03	9.57	0.10	7.31	7.08	0.23	0.13
NPCF	7.94	86.03	75.79	10.24	−0.28	29.64	28.82	0.82	1.10
DPCF	8.16	90.42	79.64	10.78	−1.46	28.71	27.92	0.79	2.25
PCP	7.86	84.44	74.40	10.04	−1.75	1.62	1.55	0.07	1.82
NPCP	8.14	90.06	79.32	10.74	−1.49	21.65	21.05	0.60	2.09
DPCP	8.35	94.30	83.04	11.26	−2.45	23.93	23.27	0.66	3.11
PCT	7.91	85.44	75.27	10.17	−2.47	3.39	3.27	0.12	2.59
NPCT	8.19	91.03	80.17	10.86	−2.40	27.04	26.29	0.75	3.14
DPCT	8.38	94.94	83.60	11.34	−3.35	25.10	24.40	0.69	4.05

With the data of $\Delta G^{*}_{W\to mix}$ and $\Delta\Delta G_c$, the Gibbs energy of solute–solvent interaction ΔG^{θ}_{int} was calculated with Eq. 9 and their values are negative in all cases with the exception of PCF (see Table 3). The numerical contribution of this quantity, in comparison with $\Delta\Delta G_c$, becomes important when the electronegativity of the heteroatom decreases (furan < pyrrole < thiophene) and with the number of nitro groups on the phenyl moiety. In fact, the highest, as absolute values, were obtained for dinitrophenylhydrazone derivatives in each family.

On the other hand, the values of G^{θ}_{nsp} calculated with Eq. 8 for each solute in each medium are negative and slightly lower (as absolute value) in 2.82 mol·L^{-1} DMSO than in W, and become more negative with the presence of nitro groups in the derivatives of thiophene, furan and pyrrole. However, the values obtained for *p*-nitro and dinitrophenylhydrazone derivatives are close (see Table 3). This is likely to be a consequence of the small difference between the polarizability values for *p*-nitro and dinitrophenylhydrazone derivatives, as well as the dipole moments, estimated at the DFT-B3LYP/6-311++G(3d,3p) level (see Table 1). As expected, the values of ΔG^{θ}_{nsp} are small and positive.

The value for the specific contribution ΔG^{θ}_{sp} (due to hydrogen bonding and/or electron donor–acceptor interactions), empirically estimated using Eq. 7, are negative in each case. However, their magnitude in absolute value is higher than the value obtained for ΔG^{θ}_{nsp}. It is very important to mention that our studies show that the hydrogen bonding constants K_{assoc} between a protic solvent such as methanol with PCT, PCF, NPCT and NPCF derivatives in benzene at 298 K, determined by means of densitometric and refractometric methods, are low in magnitude ($K_{assoc} < 1$) [46], which is evidence of the poor proton acceptor character of these phenylhydrazones. In this way, Singh and co-workers showed, by experimental and theoretical methods, that complex formation by hydrogen bonding between thiophene and methanol or DMSO (stoichiometry 1:1) is small [47]. In consequence, the high magnitude of ΔG^{θ}_{sp} may be due to other types of specific interactions such as electron donor–acceptor complexes between DMSO and phenylhydrazones, which is favored by the incremental increase of electrophilicity with the number of nitro groups on the phenyl ring [3, 4].

Also, the difference between $\Delta G^{*}_{W\to mix}$(experimental) and $\Delta G^{*}_{W\to mix}$(SPT, Eq. 10) indicates that the magnitude of ΔG^{θ}_{sp} is significant and has an important contribution to the value of $\Delta G^{*}_{W\to mix}$ in all cases. These experimental and theoretical results support the interpretation that the energy contribution from solute–solvent van der Waals interactions ΔG_{int}

to the Ben-Naim standard energy change $\Delta G^*_{W\rightarrow mix}$ are significant, but the magnitude of this property is dominated by the $\Delta\Delta G_c$ term (about 80%).

Additionally, we think that the reorganization of water H-bonds can be considered as a compensating process that does not affect the Gibbs energy change of transfer. At this point, it is noteworthy to mention that we suggest that the magnitude of $\Delta G^*_{W\rightarrow mix}$ or $\Delta\Delta G_c$ can be used as an interpretative tool for biological activity of these materials since both thermodynamic properties give information about the hydrophobic character of these solutes. The mentioned properties might determine the possible preferential interaction of these molecules with the strongly dipolar and polarizable groups in the interior of the hydrophobic cavities of the respective target sites. In fact, Klapper in 1971 [48], based on estimates of the atomic densities of six proteins, suggested that the interior of a protein is solid-like, notwithstanding its heterogeneity. Later, Richards in 1974, reached the same conclusion from atomic coordinates provided by crystal structure studies and Voronoi polyhedra [49]. In addition, Graziano has recently found that the experimental translated cavity size distribution inside globular proteins can be reproduced by means of SPT calculations [29].

The binding of drug to proteins in aqueous solutions involves the hydrophobic transfer and anchoring of the hydrated drug by formation of covalent and/or non-covalent molecular interactions. In fact, water is an essential part of the protein structure [50] and the hydrophobic hydration of the drug. So then, the water-mediated interaction between drug and a hydrophobic binding pocket of the proteins, as well as the hydrophobicity of drugs, provides the driving force underlying favorable complex formation [8, 51]. In consequence, these parameters can play an important role in apoptosis and in the biophysical chemistry of the design of new antineoplastic drugs. Interestingly, the ligand binding to biomolecules can be empirically partitioned into two contributions arising from the Gibbs energy of van der Waals interactions and cavitation Gibbs energy for the transfer of the hydrated drug into the hydrophobic pocket in the protein or a biomolecule (e.g. T lymphocytes and tubulin) [52].

In this sense, tubulin exists as a heterodimer consisting of α and β subunits which polymerize to form microtubules; this process is critical for the proper functioning of microtubules within the cell. Therefore, tubulin is an accepted target in treatments against cancer, since there are drugs that bind and stabilize these microtubules and inhibit the tubulin polymerization and trigger apoptosis (e.g. colchicine) [13]. It is very important to note that the participation of water and hydrophobic character of drugs in small-molecule binding to tubulin have not been well-characterized. Therefore, the process of creation of a cavity inside a solvent is relevant for the understanding of hydrophobic hydration and to determine the hydrophobic character of the solute.

The results obtained here about the activity to inhibit proliferation of human T lymphocytes, stimulated by phytohaemagglutinin (PHA) of selected hydrazone derivatives as a function of molecular size, are shown in Table 2. Almost all of the evaluated derivatives showed low biological activity. In spite of the complexity of these systems, these results clearly reveal a significant increment in the antiproliferative activity with both the increment of $|\Delta\Delta G_c|$ and the increment of the number of nitro groups on the phenyl ring moiety of the analyzed thiophene and furan derivatives. The antiproliferative activity follows the following order in each family of compounds: DPCT > NPCT and DPCF > NPCF. DPCT was the most-active and corresponds to the highest $|\Delta\Delta G_c|$ value (11.34 kJ·mol^{-1}). Interestingly, the value of the inhibitory activity obtained for PCT was similar to the value for DPCF but higher than the value determined for NPCT, and the magnitude of $\Delta\Delta G_c$ for PCT is very close to the value obtained for NPCF, giving a possible anomalous behavior.

Furthermore, none of the thiophene derivatives tested, with the magnitude of $\Delta\Delta G_c$ in this range, displayed inhibition of tubulin polymerization with the exception again of

the DPCT derivative, which has an IC_{50} value higher than that of the control (colchicine drug). However, the compound NPCF has a value of IC_{50} very close to that determined for DPCT. The mechanism of these compounds for inhibition of tubulin assembly apparently is complex and remains as a research line for future studies. Despite results that are not conclusive with these molecular systems, it seems like there are at least three relevant factors for the antiproliferative activity of human T-lymphocytes and inhibitory activity of tubulin polimerization. First, the mechanism of cavity formation in DMSO-containing medium; second, the transfer of the solute molecule from this cavity to the cavity in the target site, and third the high hydrophobic character of the solute.

Finally, the use of SPT (spherical model) for non-spherical molecules may seem inadequate, but we do think that random rotations of the solute in a medium give an approximately spherical cavity even when the molecules are not spherical. This is possibly the reason why excellent results are obtained in these rigid asymmetric molecular systems with this spherical model. It is clear that an implementation of more elaborate models using a spherocylindrical molecular shape as the proposed by Cotter and Martire [53], Benzi and co-workers [54], and Graziano [55] should give more detailed information about the effects of these non-specific and specific forces, and cavitation upon solvation of these materials and their role in biological activity. Studies to consider a spherocylindrical cavity for these phenylhydrazone derivatives are actually in progress in our group.

4 Conclusions

The experimental and theoretical results obtained show that the solubility of the phenylhydrazone derivatives in water diminishes with an increment in the number of nitro groups on the phenyl ring moiety in each family of compounds, and that the solubility of compounds in 2.82 mol·L^{-1} DMSO is larger than in water—in general. The corresponding value of the Gibbs energy for the dissolution process in water ΔG^0_W and in a mixture ΔG^0_{mix} is large and positive for each studied compound, and the highest absolute values were obtained for the hydrazone derivatives containing the 2,4-dinitrophenyl ring, but the values obtained in 2.82 mol·L^{-1} DMSO are lower than in water. The corresponding values of $\Delta G^0_{W\to mix}$ and $\Delta G^*_{W\to mix}$ indicate that the transfer from water to 2.82 mol·L^{-1} aqueous DMSO at 298.15 K is a spontaneous process in all of the systems considered. The value of $\Delta G^*_{W\to mix}$ might be considered a direct measurement of the interactions between the solute and DMSO molecules in the hydration shell, and in consequence, is an indirect measurement of the hydrophobic character of each phenylhydrazone derivative. In spite of the crudeness of the SPT theory, the analysis performed appears to agree with the main observations of this work, establishing that $\Delta G^*_{W\to mix}$ is practically dominated by the magnitude of the difference in the work of cavity creation $\Delta\Delta G_c$. In general, the hydrazones studied in this work show low biological activity for inhibiting the proliferation of human T-lymphocytes stimulated by phytohaemagglutinin (PHA). Furthermore, a significant increment of antiproliferative activity with the increment of both the magnitude (in absolute value) of $\Delta\Delta G_c$ and $\Delta G^*_{W\to mix}$, and the increment of the number of nitro groups on the phenyl ring moiety in the thiophene and furan derivatives was observed. In relation to the tubulin polimerization, NPCF and DPCT showed an important inhibitory activity when compared with colchicine. The rest of the thiophene derivatives were inactive. Apparently, the biological activities of these compounds are directly related to their hydrophobicity.

Acknowledgements The authors thank to the *Fondo Nacional de Ciencia, Tecnología e Innovación* (FONACIT, *Proyecto de apoyo a Grupos* No. G-2005000403), *Instituto Zuliano de Investigaciones Tecnológicas* (INZIT), CONDES-LUZ, *Avícola La Rosita S. A.* and *Petroregional del Lago S. A.* (PERLA) for partial financial support of this work. The authors thank Dr. Juan Chirinos Colina for his help in the discussion of this manuscript, and the referees for important observations and very helpful comments on the present work.

References

1. Rollas, S., Küçükgüzel, S.G.: Biological activities of hydrazone derivatives. Molecules **12**(8), 1910–1939 (2007)
2. Kalinowski, D.S., Richardson, D.R.: The evolution of iron chelators for the treatment of iron overload disease and cancer. Pharmacol. Rev. **57**(4), 547–583 (2005)
3. Morgan, L.R., Thangaraj, K., LeBlanc, B., Rodgers, A., Wolford, L.T., Hooper, C.L., Fan, D., Jursic, B.S.: Design, synthesis, and anticancer properties of 4,4′-dihydroxybenzophenone-2,4-dinitrophenylhydrazone and analogues. J. Med. Chem. **46**(21), 4552–4563 (2003)
4. Morgan, L.R., Jursic, B.S., Hooper, C.L., Neumann, D.M., Thangaraj, K., LeBlanc, B.: Anticancer activity for 4,4′-dihydroxybenzophenone-2,4-dinitrophenylhydrazone (A-007) analogues and their abilities to interact with lymphoendothelial cell surface markers. Bioorg. Med. Chem. Lett. **12**(23), 3407–3411 (2002)
5. Sagiraju, S., Jursic, B.S.: NMR spectroscopic study of cyclodextrin inclusion complexes with A-007 prodrugs. Carbohydr. Res. **343**(7), 1180–1190 (2008)
6. Miyamoto, S., Kollman, P.A.: What determines the strength of noncovalent association of ligands to proteins in aqueous solution? Proc. Natl. Acad. Sci. USA **90**(18), 8402–8406 (1993)
7. Alvarado, Y.J., Caldera-Luzardo, J., Ferrer-Amado, G., Manzilla-Labarca, V., Michelena, E.: Determination of the apparent molar refraction and partial molar volume at infinite dilution of thiophene-, pyrrole- and furan-2-carboxaldehyde phenylhydrazone derivatives in acetonitrile at 293.15 K. J. Solution Chem. **36**(1), 1–11 (2007)
8. Wang, H., Ben-Naim, A.: A possible involvement of solvent-induced interactions in drug design. J. Med. Chem. **39**(7), 1531–1539 (1996)
9. Santos, N.C., Figueira-Coelho, J., Martins-Silva, J., Saldanha, C.: Multidisciplinary utilization of dimethyl sulfoxide: pharmacological, cellular, and molecular aspects. Biochem. Pharmacol. **65**(7), 1035–1041 (2003)
10. Alvarado, Y.J., Baricelli, J., Caldera-Luzardo, J., Cubillán, N., Ferrer-Amado, G., Marrero-Ponce, Y., Mancilla, V., Rocafull, M.A., Ojeda-Andara, J., Thomas, L.E., Vera-Villalobos, J., Morales-Toyo, M.: Thermodynamics of solution, interaction with calf thymus DNA and anticancer activity of phenylhydrazone derivatives. J. Solution Chem. (2010, in press)
11. Kuo, Y.C., Weng, S.C., Chou, C.J., Chang, T.T., Tsai, W.J.: Activation and proliferation signals in primary human T lymphocytes inhibited by ergosterol peroxide isolated from *Cordyceps cicadae*. Br. J. Pharmacol. **140**(5), 895–906 (2003)
12. Lin, C., Hamel, E.: Effects of inhibitors of tubulin polymerization on GTP hydrolysis. J. Biol. Chem. **256**(17), 9242–9245 (1981)
13. Morgan, R.E., Ahn, S., Nzimiro, S., Fotie, J., Phelps, M.A., Cotrill, J., Yakovich, A.J., Sackett, D.L., Dalton, J.T., Werbovetz, K.A.: Inhibitors of tubulin assembly identified through screening a compound library. Chem. Biol. Drug Des. **72**(6), 513–524 (2008)
14. Cullen, M.D., Sarkar, T., Hamel, E., Hartman, T.L., Watson, K.M.: Jr., R. W. B., Pannecouque, C., Clercq, E. D., Cushman, M., Inhibition of tubulin polymerization by select alkenyldiarylmethanes. Bioorg. Med. Chem. Lett. **18**(2), 469–473 (2008)
15. Pierotti, R.A.: A scaled particle theory of aqueous and nonaqueous solutions. Chem. Rev. **76**(6), 717–726 (1976)
16. Graziano, G.: Solvation thermodynamics of water in nonpolar organic solvents indicate the occurrence of nontraditional hydrogen bonds. J. Phys. Chem. B **109**(2), 981–985 (2005)
17. Graziano, G.: Hydration thermodynamics of N-methylacetamide. J. Phys. Soc. Jpn. **69**(11), 3720–3725 (2000)
18. Soscún, H., Alvarado, Y., Hernández, J., Hernández, P., Atencio, R., Hinchliffe, A.: Experimental and theoretical determination of the dipole polarizability of dibenzothiophene. J. Phys. Org. Chem. **14**(10), 709–715 (2001)
19. Alvarado, Y.J., Cubillán, N., Labarca, H.P., Karam, A., Arrieta, F., Castellano, O., Soscún, H.: Dipole polarizability of the pyrazabole molecule in solution. J. Phys. Org. Chem. **15**(12), 835–843 (2002)

20. Alvarado, Y., Cubillán, N., Labarca, H.P., Karam, A., Arrieta, F., Castellano, O., Soscún, H.: Static and dynamic dipole polarizabilities of 2- and 3-methylthiophenes in solution: experimental and theoretical determination. J. Phys. Org. Chem. **15**(3), 154–164 (2002)
21. Alvarado, Y.J., Labarca, H.P., Cubillán, N., Osorio, E., Karam, A.: Solvent effect on electronic polarizability of benzonitrile. Z. Naturforsch. **58a**(2), 68–74 (2003)
22. Alvarado, Y.J., Caldera-Luzardo, J., De La Cruz, C., Ferrer-Amado, G., Michelena, E., Silva, P.: Volumetric, electric, and magnetic properties of thioxanthen-9-one in aprotic solvents as revealed by high-precision densitometry, high-accuracy refractometry and magnetic susceptibility measurements and by DFT calculations. J. Solution Chem. **35**(1), 29–49 (2006)
23. Zielenkiewicz, W., Golankiewicz, B., Perlovich, G.L., Kozbial, M.: Aqueous solubilities, infinite dilution activity coefficients and octanol-water partition coefficients of tricyclic analogs of Acyclovir. J. Solution Chem. **28**(6), 731–745 (1999)
24. Liu, Z., Weng, W., Bookchin, R.M., Lew, V.L., Ferrone, F.A.: Free energy of sickle hemoglobin polymerization: a Scaled-Particle treatment for use with dextran as a crowding agent. Biophys. J. **94**(9), 3629–3634 (2008)
25. Segatin, N., Klofutar, C.: Thermodynamics of solution of some alkyl acetates in water. Monatsh. Chem. **132**(12), 1451–1462 (2001)
26. Graziano, G.: On the solubility of aliphatic hydrocarbons in 7 M aqueous urea. J. Phys. Chem. B **105**(13), 2632–2637 (2001)
27. Ben-Naim, A.: Solvation Thermodynamics. Elsevier, Amsterdam (1987)
28. Graziano, G.: Size and temperature dependence of hydrocarbon solubility in concentrated aqueous solutions of urea and guanidine hydrochloride. Can. J. Chem. **80**(4), 388–400 (2002)
29. Graziano, G.: Cavity size distribution in the interior of globular proteins. Chem. Phys. Lett. **434**(4–6), 316–319 (2007)
30. Graziano, G.: Solvation thermodynamics of methane and ethane in dimethyl sulfoxide and acetone versus water. Chem. Phys. Lett. **449**(1–3), 120–125 (2007)
31. Riddle, F., Fowkes, F.: Spectral shifts in acid-base chemistry. 1. Van der Waals contributions to acceptor numbers. J. Am. Chem. Soc. **112**(9), 3259–3264 (1990)
32. Quin, Y., Prausnitz, J.M.: Solubilities in ionic liquids and molten salts from a simple Perturberd-Hard-Sphere theory. Ind. Eng. Chem. Res. **45**(16), 5518–5523 (2006)
33. Barford, W., Xu, X.: Groundstate dispersion interaction between π-conjugated polymers. J. Chem. Phys. **128**, 034705 (2008)
34. Stolypin, V.F., Mishustin, A.L.: Calculation of the contribution from van der Waals interactions to the thermodynamic properties of binary mixtures of dipolar aprotic solvents. Russ. J. Phys. Chem. **61**, 1703–1705 (1987)
35. McLain, S.E., Soper, A.K., Luzar, A.: Investigations on the structure of dimethyl sulfoxide and acetone in aqueous solution. J. Chem. Phys. **127**, 174515 (2007)
36. Librando, L., Alparone, A.: The role of electronic properties to the mutagenic activity of 1,6- and 3,6-dinitrobenzo[a]pyrene isomers. J. Hazard. Mater. **161**(2–3), 1338–1346 (2009)
37. Suppan, P., Ghoneim, N.: Solvatochromism. The Royal Society of Chemistry, London (1997)
38. Wong, M.W., Wiberg, K.B., Frisch, M.J.: Ab initio calculation of molar volumes: Comparison with experimental and use in solvation models, *J. Comp. Chem.* **16**(3), 385–394 (1995)
39. Frisch, M.J., Trucks, G.W., Schlegel, H.B., Scuseria, G.E., Robb, M.A., Cheeseman, J.R., Montgomery, J.A. Jr., Vreven, T., Kudin, K.N., Burant, J.C., Millam, J.M., Iyengar, S.S., Tomasi, J., Barone, V., Mennucci, B., Cossi, M., Scalmani, G., Rega, N., Petersson, G.A., Nakatsuji, H., Hada, M., Ehara, M., Toyota, K., Fukuda, R., Hasegawa, J., Ishida, M., Nakajima, T., Honda, Y., Kitao, O., Nakai, H., Klene, M., Li, X., Knox, J.E., Hratchian, H.P., Cross, J.B., Bakken, V., Adamo, C., Jaramillo, J., Gomperts, R., Stratmann, R.E., Yazyev, O., Austin, A.J., Cammi, R., Pomelli, C., Ochterski, J.W., Ayala, P.Y., Morokuma, K., Voth, G.A., Salvador, P., Dannenberg, J.J., Zakrzewski, V.G., Dapprich, S., Daniels, A.D., Strain, M.C., Farkas, O., Malick, D.K., Rabuck, A.D., Raghavachari, K., Foresman, J.B., Ortiz, J.V., Cui, Q., Baboul, A.G., Clifford, S., Cioslowski, J., Stefanov, B.B., Liu, G., Liashenko, A., Piskorz, P., Komaromi, I., Martin, R.L., Fox, D.J., Keith, T., Al-Laham, M.A., Peng, C.Y., Nanayakkara, A., Challacombe, M., Gill, P.M.W., Johnson, B., Chen, W., Wong, M.W., Gonzalez, C., Pople, J.A.: Gaussian 03, Revision D.02. Gaussian, Inc., Wallingford (2004)
40. Boyum, A.: Separation of leucocytes from blood and bone marrow. Scand. J. Clin. Lab. Invest. **21**(Suppl. 97), 310–350 (1968)
41. Fuss, I.J., Kanof, M.E., Smith, P.D., Zola, H.: Isolation of whole mononuclear cells from peripheral blood and cord blood. Curr. Protoc. Immunol. **19**(Unit 7.1) (1996)
42. Fiocchi, C., Youngman, K.R.: Isolation of human intestinal mucosal mononuclear cells. Curr. Protoc. Immunol. **19**(Unit 7.3) (1996)
43. Strober, W.: Monitoring cell growth. Curr. Protoc. Immunol. **21**(Appendix 3A) (1997)

44. Mobley, J.L., Shimizu, Y.: Measurement of cellular adhesion under static conditions. Curr. Protoc. Immunol. **11**(Unit 7.28) (1994)
45. Hamel, E.: Antimitotic natural products and their interactions with tubulin. Med. Res. Rev. **16**(2), 207–231 (1996)
46. Alvarado, Y.J., Cubillán, N.: Manuscript in preparation (2010)
47. Singh, D.K., Srivastava, S.K., Ojha, A.K., Asthana, B.P.: Vibrational study of thiophene and its solvation in two polar solvents, DMSO and methanol by Raman spectroscopy combined with ab initio and DFT calculations. J. Mol. Struct. **892**(1–3), 384–391 (2008)
48. Klapper, M.H.: On the nature of the protein interior. Biochim. Biophys. Acta. **229**(3), 557–566 (1971)
49. Richards, F.M.: The interpretation of protein structures: total volume, group volume distributions and packing density. J. Mol. Biol. **82**(1), 1–14 (1974)
50. Ball, P.: Water as an active constituent in cell biology. Chem. Rev. **108**(1), 74–108 (2008)
51. Valdez, R., Johnson, E.M., Belcher, J.A., Fuini, J.F. III, Brancaleon, L.: Porphyrins affect the self-assembly of tubulin in solution. Biophys. Chem. **145**(2–3), 98–104 (2008)
52. Olson, M.A., Cuff, L.: Free energy determinants of binding the rRNA substrate and small ligands to Ricin A-Chain. Biophys. J. **76**(1), 28–39 (1999)
53. Cotter, M.A., Martire, D.E.: Statistical mechanics of rodlike particles. II. A Scaled Particle investigation of the aligned → isotropic transition in a fluid of rigid spherocylinders. J. Chem. Phys. **52**(4), 1970 (1909–1919) ()
54. Benzi, C., Cossi, M., Improta, R., Barone, V.: Building cavities in a fluid of spherical or rod-like particles: a contribution to the solvation free energy in isotropic and anisotropic polarizable continuum model. J. Comput. Chem. **26**(11), 1096–1105 (2005)
55. Graziano, G.: Dimerization thermodynamics of large hydrophobic plates: a scaled particle theory study. J. Phys. Chem. B **113**(32), 11232–11239 (2009)